Sub Topic: Turbulent Flames

11th U.S. National Combustion Meeting
Organized by the Western States Section of the Combustion Institute
March 24–27, 2019
Pasadena, California

# DNS of a turbulent premixed flame stabilized over a backward facing step

*Konduri Aditya*[1,*], *Hemanth Kolla*[1], *and Jacqueline H. Chen*[1]

[1] *Sandia National Laboratories, Livermore CA, USA*
[*] *Corresponding author:* `konduri.adi@gmail.com`

**Abstract:** Flame stabilization in practical combustors is often achieved through recirculation zones created due to geometrical effects. Direct numerical simulation of a premixed flame in a backward facing step configuration is performed to study the flame stabilization mechanism and the turbulent flame structure. A lean ethylene-air mixture at conditions relevant to scramjet combustion is introduced at the domain inlet. Simulation results show that a recirculation zone, established downstream of the step, transports key radicals to the edge of the step where flame stabilization is established. The flame structure is affected by the transport of the wall- and shear-generated turbulence from the reactant to the product side of the flame, which enhances mixing on the product side and results in enhanced heat transfer to the wall. Statistics of the enstrophy budget as a function of progress variable and streamwise distance are presented to quantify the vorticity transport. The flame structure resulting from its interaction with sheared turbulence and the recirculation zone is studied as a function of streamwise distance. The flame structure is found to be affected by turbulent strain resulting in partial quenching of the oxidation layer immediately behind the step and reliance of radicals produced downstream and transported upstream via recirculation to sustain the flame. Downstream reactions are able to complete as the strain rate relaxes.

***Keywords:* Premixed, turbulent flames, backward facing step, DNS**

## 1. Introduction

Scramjet combustors, which possess short flow residence time, use recirculation zones for flame stabilization. The recirculation zones provide the necessary pool of radicals and enthaply to stabilize flames in the low velocity regions of shear layers. Among different geometries, cavity flame holders are often used in scramjet engines. Several experimental and numerical studies have been conducted to understand the stabilization mechanism, flame structure and combustion dynamics [1, 2]. Recently, experiments in a down-scaled cavity flame holder have been performed at the University of Virgnia Supersonic Combustion Facility (UVaSCF) [3] to facilitate comparison with realizable direct numerical simulations (DNS) using existing computational power. The experiments introduce ethylene fuel into the combustor which mixes well with the free stream air to form lean premixed reactants. The reactants are then consumed by a stable flame anchored at the leading edge of the cavity flame holder. As a complementary effort, a multi-block geometry capability has recently been developed in Sandia's S3D DNS solver [4] to enable reacting flow simulations in a rectangular cavity domain [5]. In addition, an immersed boundary method (IBM) has been implemented to impose a linear ramp on the aft end of the cavity that enables the computational domain to be nidentical to the experimental setup [6].

With the experimentally relevant geometry and high speed flow conditions, simulations of the cavity flow are complex and demand massive computations. Hence, a DNS of a simpler backward facing step configuration at a relatively lower speed is attempted first in this study. This configuration is also relevant to flame anchoring in sequential stationary gas turbine engines, particularly in reheat combustors [5, 7]. This present study, to the best of our knowledge, is the first DNS in this geometry which provides detailed insights into the role of the recirculation zone and shear layer in flame stabilization and the downstream evolution of the flame structure.

The remainder of the paper is organized as follows. The simulation details of the lean ethylene-air premixed flame in the backward facing step configuration are provided in section 2. Results on the flame stabilization mechanism, flame-vorticity interactions and flame structure are presented in section 3 and conclusions are discussed in section 4.

## 2. Simulation details

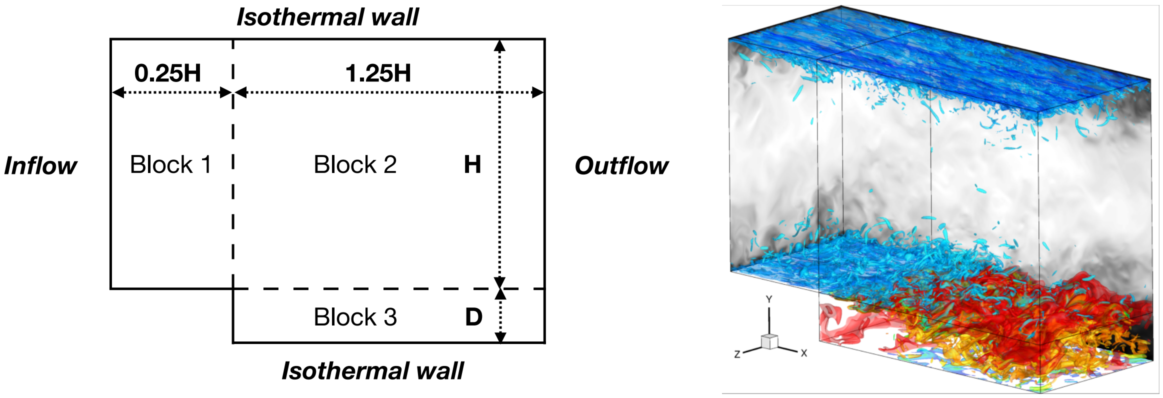

Figure 1: *Left*: A schematic of the DNS domain. *Right*: Illustration of the instantaneous flow field represented by iso-surfaces of vorticity magnitude colored by the temperature scale. The flame is illustrated by the red iso-surface of a representative value of heat release rate. The gray scale represents the magnitude of the streamwise component of velocity.

The simulation in the backward facing step configuration is enabled by the multi-block version of S3D (S3D-MB) with the domain decomposed into multiple computational blocks, as shown in Figure 1. The geometry consists of an inlet channel (Block 1), followed by a sudden expansion due to the step (Blocks 2 and 3). The relative dimensions in the streamwise and transverse directions are shown in the figure. The height of the inlet channel ($H$) and the step ($D$) are 1.466$cm$ and 0.3048$cm$, respectively, which match the experimental setup in [2]. The spanwise length is 1$cm$. The S3D-MB code solves the governing conservation equations in the compressible formulation and preserves the numerical accuracy of the base code. The time integration is performed with an explicit six-stage 4th-order Runge-Kutta method, while the spatial derivatives are computed with 8th-order central difference schemes [8]. A 10th-order filter is applied to the solution at each time step to remove spurious oscillation.

A turbulent velocity profile, generated from an auxiliary DNS of a periodic channel, with a non-reflecting Navier-stokes characteristic boundary condition (NSCBC) treatment is imposed at the inflow. The inflow bulk velocity is $200 m/s$, which has a Mach number of 0.3 and a Reynolds number $Re_\tau = 790$. The inflow consists of a premixed mixture of ethylene-air at an equivalence ratio of 0.42 and a temperature of $1125K$. The walls in the domain are maintained at a constant temperature of $600K$, and no-slip, no penetration conditions are imposed for the velocity components. The outflow boundary condition is set by the non-reflecting NSCBC outflow. A periodic boundary condition is imposed along the spanwise direction. The ambient pressure in the simulation is set to $1.72 atm$. A uniform grid size of $24\mu m$ is used in the streamwise and spanwise directions. In the transverse direction, a non-uniform grid with $24\mu m$ in the near-wall region that stretches to $40\mu m$ along the centerline of the channel is used. The grid resolution sufficiently resolves the flame and captures the near-wall structures. Overall, the grid consists of 350 million points. The ethylene-air chemistry is represented with a 22-species reduced mechanism from Z. Lou et al. [9].

A statistically stationary turbulent premixed flame is established in the domain with the following steps. First, the flow in the domain is initialized with a non-reacting laminar solution obtained from a 2D simulation that is extruded in the spanwise direction. With a turbulent inflow condition, the simulation is evolved in time for 4 flow-through times to obtain a nearly statistically steady non-reacting turbulent flow. A laminar flame is then imposed near the step region of Block 3. With time the flame propagates under the influence of turbulence and stabilizes near the step corner. The solution is evolved for 4 more flow-through times before statistics are accumulated to analyze the flow-flame interaction.

## 3. Results

An instantaneous flow field with a stabilized flame in the backward facing step geometry is shown in Figure 2. The isocontour plots in the figure show the flame anchored near the step corner and extending downstream in the shear layer. Due to the high inflow speed the flame does not propagate towards the center of the channel and remains nearly parallel to the streamwise direction. The dilatation at the flame surface inhibits the channel flow from rapidly expanding into the bottom of the cavity, and thus the flame is not significantly affected by the channel turbulence. Negative values of the streamwise velocity component are observed in the expansion region which are representative of the recirculation zone. The temperature of the products is greater closer to the step and decreases downstream. To aid further in the analysis of the flame stabilization, the interaction of the flame with the shear layer and its flame structure, a progress variable ($c$) is defined based on the mass fraction of $O_2$ as:

$$c = \frac{y_{O_2} - y^u_{O_2}}{y^b_{O_2} - y^u_{O_2}} \tag{1}$$

where the superscripts $u$ and $b$ represent the unburnt and burnt mass fractions, respectively.

### 3.1 Flame stabilization

To understand the flame stabilization, isocontours of mean reaction rate of OH, which is a key radical produced in the oxidation layer of the flame, are shown in the left panel of Figure 3. The contours show significant production of OH downstream, and primarily consumption near the flame stabilization point at the edge of the step. The mean streamlines in the figure show the presence

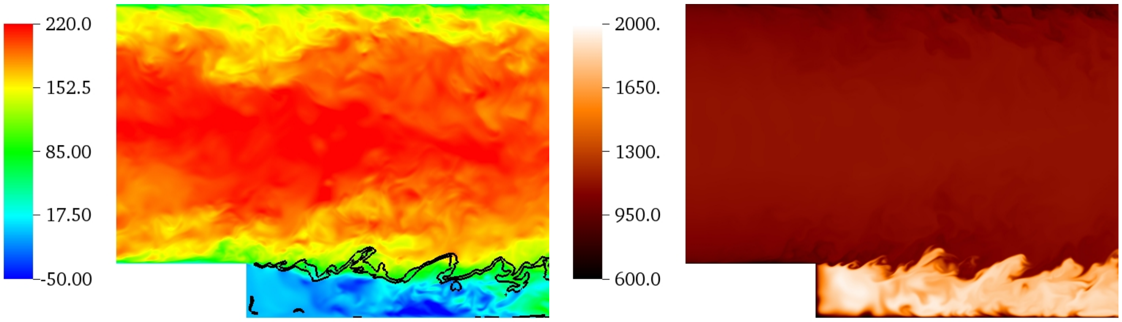

Figure 2: *Left*: Instantaneous contours of streamwise component of velocity (m/s) at the midplane. The black iso-lines of heat release rate represents the flame. Right: Instantaneous contours of temperature ( K) at the midplane.

of a recirculation zone that entrains OH and other key radicals produced downstream of the step, and transports them upstream. Profiles of the mean reaction rate of OH conditioned on progress variable at selected streamwise locations are shown in the right panel of Figure 3. Near the stabilization point OH is primarily consumed at a value of progress value close to 0.7 closer to the burnt side. Moving downstream, OH production occurs at successively lower values of progress variable, while OH consumption rate increases and also shifts to lower progress variable values. The downstream evolution of the conditional OH reaction rate is consistent with previous observations in a piloted turbulent premixed jet flame [10] wherein high turbulent strain rates in the near field of the jet suppresses radical production in the oxidation layer of the flame and the flame's reaction zone is pushed into the product gases where it relies on transport of OH from the pilot to support OH consumption by the flame in the nearfield. As the strain rate relaxes downstream in the jet CO and H2 oxidation produce OH radicals, OH consumption increases, and the flame position shifts back towards the reactant stream. The transport of OH radicals due to the recirculation zone is evident from the contours of streamwise and transverse flux of OH, shown in Figure 4. A negative streamwise flux near the bottom wall and a positive transverse flux closer to the step illustrate the transport of radicals to stabilize the flame. Similar trends are also seen in the flux contours of other key radicals and temperature (not shown here). In time, the flame base/tip oscillates slightly near the step corner which can be attributed to the vortex shedding arising from the corner.

### 3.2 Flame-vorticity interactions

With a high speed inflow provided by a fully developed channel simulation, significant shear and high values of enstrophy are generated in the near-wall region. The shear layer that emanates from the step provides an additional source of enstrophy production. However, heat release at the flame dissipates the vortical structures, especially towards the burnt side. To understand these competing effects, instantaneous isocontours of enstrophy and mean enstrophy conditioned on the progress variable at different streamwise locations are illustrated in Figure 5. The isocontours in the figure show, as mentioned before, high enstrophy in the near-wall region. Downstream of the step, enstrophy is significant in the shear layer and interacts with the flame. Note that near the step vortical structures are present on the reactant side of the flame, and shift to predominantly the product side downstream. This is also evident from the conditional mean plot showing the peak

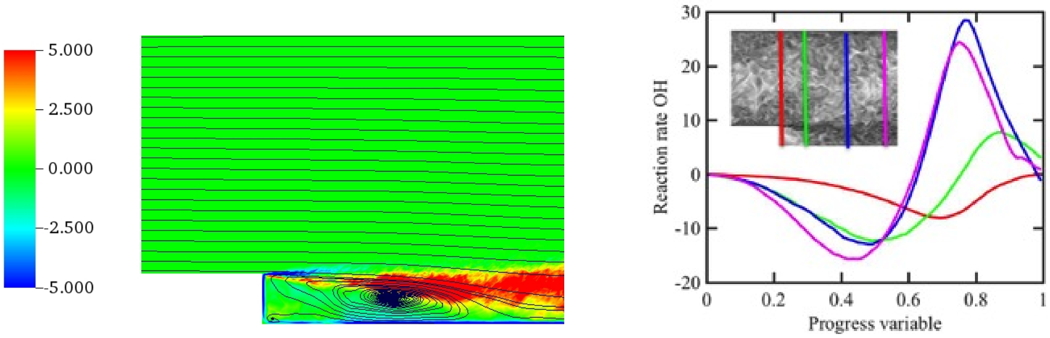

Figure 3: *Left*: Mean isocontours of reaction rate of OH superimposed onto mean streamlines of the flow. *Right*: Conditional mean reaction rate of OH as a function of progress variable at different streamwise locations.

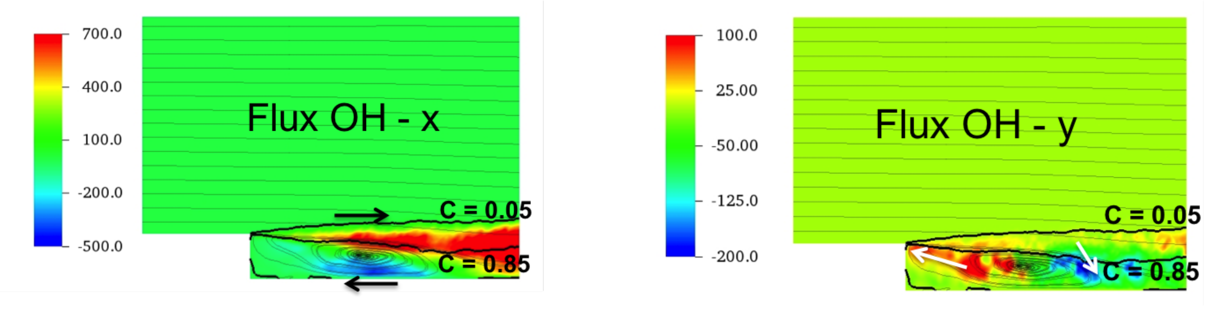

Figure 4: Mean isocontours of OH flux along the streamwise and transverse directions. The thin black lines represent the mean streamlines. For reference isolines of low and high values of the progress variable (thick black lines) demarcate the flame brush location.

enstrophy at low values of progress variable near the step and a shift of the peak towards higher values of progress variable downstream. The relative magnitude of peak enstrophy decays with downstream distance which is likely due to the effect of viscous dissipation.

To analyze the processes responsible for the observed dynamics, consider the enstrophy transport equation,

$$\frac{\partial}{\partial t}\left(\frac{\omega^2}{2}\right)+\underbrace{u_i\frac{\partial}{\partial x_i}\left(\frac{\omega^2}{2}\right)}_{\text{Advection}}=\underbrace{\omega_i\omega_j\frac{\partial u_i}{\partial x_j}}_{\substack{\text{Vortex}\\\text{stretching}}}\underbrace{-\,\omega^2\frac{\partial u_j}{\partial x_j}}_{\text{Dilatation}}+\underbrace{\frac{\omega_i}{\rho^2}\varepsilon_{ijk}\frac{\partial \rho}{\partial x_j}\frac{\partial P}{\partial x_k}}_{\substack{\text{Baroclinic}\\\text{torque}}}+\underbrace{\omega_i\varepsilon_{ijk}\frac{\partial}{\partial x_j}\left(\frac{1}{\rho}\frac{\partial \tau_{kl}}{\partial x_l}\right)}_{\text{Dissipation}}, \qquad (2)$$

where $\omega^2$ is the enstrophy, $u_i$ is the velocity component, $\rho$ is the density, $P$ is the pressure and $\tau_{kl}$ is the stress tensor component. The mean of the terms from the enstrophy transport equation are presented in Figure 6. Near the step (left plot) enstrophy production is mainly due to the vortex stretching term, while dilatation and viscous dissipation terms deplete enstrophy at low values of the progress variable. At this location the advection term is also significant with a negative sign, which causes the advection of vortex structures from the reactant to the product side of the flame. The contribution from baroclinic torque remains insignificant. With downstream distance, the magnitude of the budget terms decreases and the peak values shift to higher progress variable,

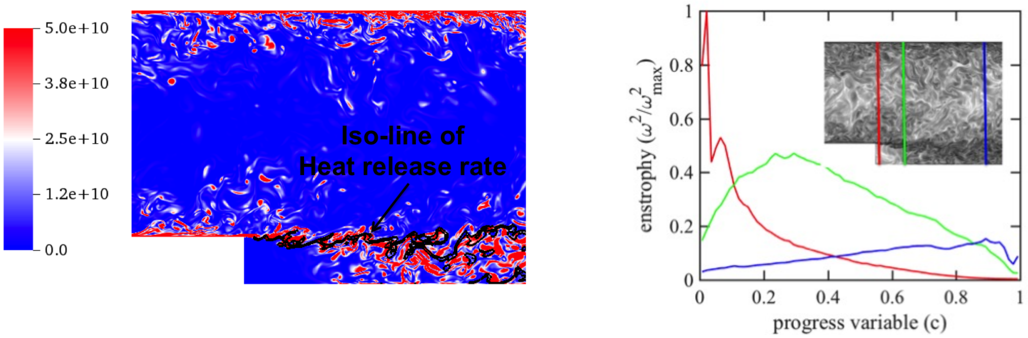

Figure 5: *Left*: Instantaneous isocontours of enstrophy with iso-lines of heat release rate superimposed. *Right*: Mean enstrophy conditioned on progress variable at different streamwise locations.

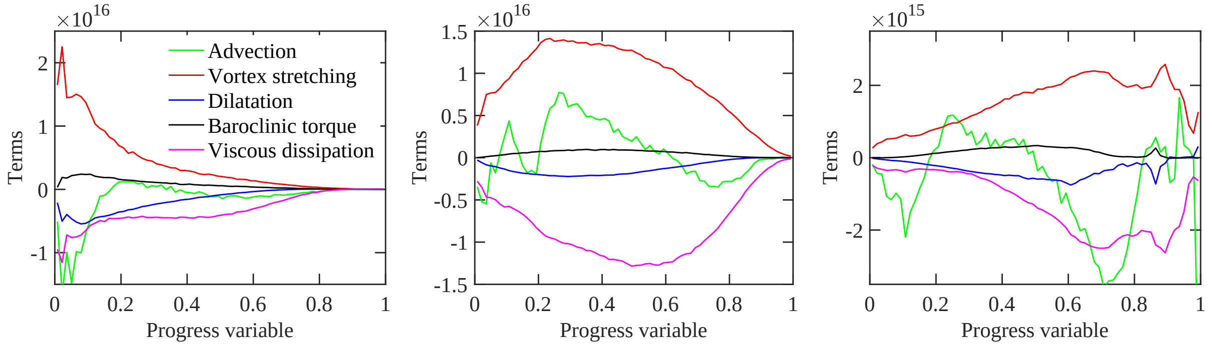

Figure 6: Budget of the enstrophy transport equation conditioned on the progress variable at different streamwise locations (same location sequence as in Figure 5).

similar to the observation in Figure 5. The physical mechanism and the flow structures responsible for the transport of enstrophy from the reactants to the products is currently under investigation.

The presence of enstrophy on the product side of the flame could affect its oxidation layer if the turbulence is strong enough to compete with CO and H2 oxidation rates. However, since turbulence is significantly dissipated downstream and the peak in enstrophy is substantially lower than immediately behind the step, it is more likely that CO and H2 oxidation will go to completion due to the increase in residence time downstream. In addition, the vortex structures on the product side increase the transverse mixing and enhance the heat loss to the cold isothermal walls. This is illustrated by the rise in the (negative) heat flux at the wall downstream, with greater enstrophy near the walls as seen in the contours of Figure 5.

### 3.3 Flame structure

Instantaneous iso-lines of the progress variable at different values in a spanwise midplane are show in Figure 8, with isocontours of enstrophy in the background. Near the stabilization point the sheared turbulence wrinkles the flame and small-scale turbulence broadens the preheat zone of the flame. Downstream as the turbulence migrates towards the burnt side of the flame, the oxidation layer is broadened, leading to more distributed reactions occurring in the oxidation layer while the preheat layer is largely unperturbed. Isocontours of formaldehyde mass fraction, which is produced

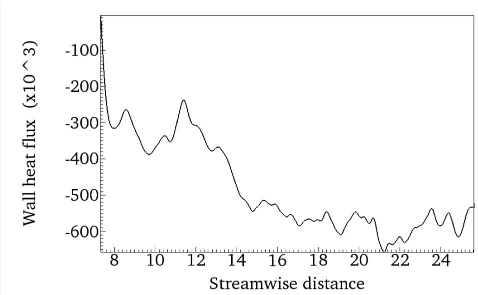

Figure 7: Instantaneous heat flux at the bottom isothermal wall downstream of the step.

in the flame and persists thereby serving as a marker for the preheat zone, show substantial flame-flame interaction in Figure 9. The effect of the transient flame-flame interaction as a potential source of increased radicals is being investigated currently. The increase in OH radicals (right panel of Figure 9) downstream suggests that the oxidation reactions are able to complete due to the relaxation of strain rates as turbulence dissipates downstream, assisted by increased mixing with hot burnt products.

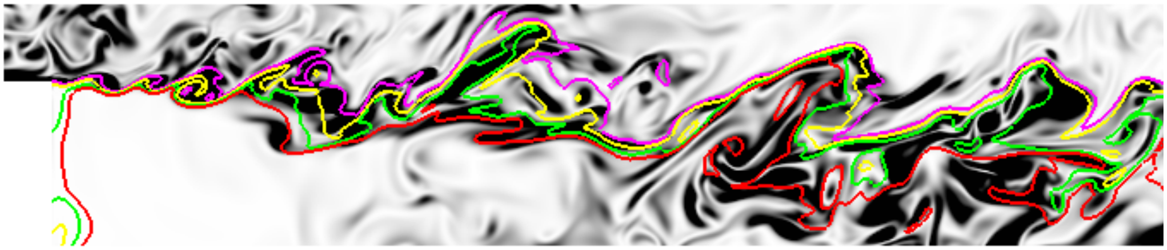

Figure 8: Instantaneous iso-line of progress variable (magenta: 0.2, yellow: 0.5, green: 0.8, red: 0.9) with contours of enstrophy in the background (black: higher value).

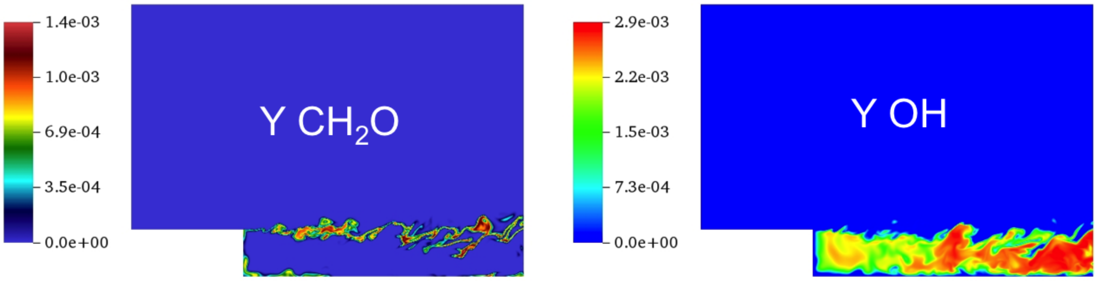

Figure 9: Instantaneous contours of mass fraction of $HO_2$ and $OH$.

Further evidence on the influence of turbulent strain and flow recirculation on the downstream evolution of the flame structure is shown by the conditional mean reaction rate plots of C2H4, CO, OH, HO2, heat release rate and the magnitude of the gradient of the progress variable (measure of the flame thickness) in Figure 10. Similar to the downstream development in the piloted premixed jet flame under intense sheared turbulent conditions [10] we observe the CO and H2 oxidation reactions responsible for radical production (OH, H and O) are affected near the step such that CO and H2 production is quenched and these reactions operate in reverse, producing a tiny amount of OH rather than H. The flame is sustained there mainly by transport of radicals produced downstream of the step by flow recirculation. Hence, fuel oxidation and heat release remain active albeit reduced. Under high strain rates the reaction zone resides in the products and as the strain rate relaxes downstream the flame migrates back to its normal position as shown in the shift in the peak C2H4 consumption rate and heat release rate to lower values of progress variable with downstream distance. Finally, the reaction rates increase with downstream distance assisted by the increase in residence time and by the transport of heat and stable intermediates from upstream. Finally, the flame thinning in the preheat zone (low values of progress variable) is evident immediately behind the step where the strain rates are high, and flame broadening especially of the oxidation layer is evident downstream as the turbulence is transported to the product side.

## 4. Conclusions

A direct numerical simulation of a lean ethylene-air turbulent premixed flame in a backward facing step configuration was performed to study the flame stabilization and flame structure interaction with the shear layer and flow recirculation relevant to scramjet engine conditions. A detailed model with 22-species was used to represent the ethylene-air chemistry. Results show that a recirculation zone created due the sudden expansion at the step stabilizes the flame near the edge of the step. The stabilization mechanism has been studied by analyzing the production and consumption of the OH radical together with its transport due the recirculation. The near-wall vortical structures which are generated on the reactant side of the flame near the stabilization point advect into the product side downstream. This was shown to have significant impact on the heat loss to the wall and on enhanced mixing within the oxidation layer. The flame structure, under the influence of sheared turbulence and large-scale flow recirculation, is found to vary significantly in the streamwise direction.

Another direct numerical simulation with a greater streamwise domain length and higher spatial resolution is currently under progress. The simulation will provide improved convergence in the statistics.

## 5. Acknowledgements

This work at Sandia National Laboratories was supported by the US Department of Energy, Office of Basic Energy Sciences, Division of Chemical Sciences, Geosciences, and Biosciences. Sandia National Laboratories is a multimission laboratory managed and operated by National Technology and Engineering Solutions of Sandia, LLC., a wholly owned subsidiary of Honeywell International, Inc., for the US Department of Energy's National Nuclear Security Administration under contract DE-NA-0003525. The views expressed in the article do not necessarily represent the views of the U.S. Department of Energy or the United States Government. The computational allocation for the present study was provided by the National Energy Research Scientific Computing Center (NERSC) at Lawrence Berkeley National Laboratory and by the National Center for Computational Sciences at Oak Ridge National Laboratory.

## References

[1] J. Urzay, Supersonic Combustion in Air-Breathing Propulsion Systems for Hypersonic Flight, Annual Review of Fluid Mechanics 50 (2018) 593–627.

[2] R. D. Rockwell, C. P. Goyne, H. Chelliah, J. C. McDaniel, B. E. Rice, J. R. Edwards, L. M. L. Cantu, E. C. A. Gallo, A. D. Cutler, and P. M. Danehy, Development of a Premixed Combustion Capability for Dual-Mode Scramjet Experiments, Journal of Propulsion and Power 34 (2017) 438–448.

[3] T. Nielsen, J. R. Edwards, H. K. Chelliah, D. A. Lieber, C. M. Geipel, C. P. Goyne, R. D. Rockwell, and A. D. Cutler, “Hybrid LES/RANS Simulation of a Premixed Ethylene-fueled Dual-mode Scramjet Combustor: Small Cavity Configuration”, in: AIAA Scitech 2019 Forum, American Institute of Aeronautics and Astronautics, 2019.

[4] J. H. Chen, A. Choudhary, B. de Supinski, M. DeVries, E. R. Hawkes, S. Klasky, W. K. Liao, K. L. Ma, J. Mellor-Crummey, N. Podhorszki, R. Sankaran, S. Shende, and C. S. Yoo, Terascale direct numerical simulations of turbulent combustion using S3D, Computational Science & Discovery 2 (2009) 015001.

[5] K. Aditya, A. Gruber, C. Xu, T. Lu, A. Krisman, M. R. Bothien, and J. H. Chen, Direct numerical simulation of flame stabilization assisted by autoignition in a reheat gas turbine combustor, Proceedings of the Combustion Institute 37 (2019) 2635–2642.

[6] A. H. Rauch, A. Konduri, J. Chen, H. Kolla, and H. K. Chelliah, “DNS Investigation of Cavity Stabilized Premixed Turbulent Ethylene-Air Flame”, in: 2018 AIAA Aerospace Sciences Meeting, American Institute of Aeronautics and Astronautics, 2018.

[7] M. A. Nemitallah, G. Kewlani, S. Hong, S. J. Shanbhogue, M. A. Habib, and A. F. Ghoniem, Investigation of a turbulent premixed combustion flame in a backward-facing step combustor; effect of equivalence ratio, Energy 95 (2016) 211–222.

[8] C. A. Kennedy and M. H. Carpenter, Several New Numerical Methods for Compressible Shear-Layer Simulations, Applied Numerical Mathematics 14 (1994) 397–433.

[9] Z. Luo, C. S. Yoo, E. S. Richardson, J. H. Chen, C. K. Law, and T. Lu, Chemical explosive mode analysis for a turbulent lifted ethylene jet flame in highly-heated coflow, Combustion and Flame 159 (2012) 265–274.

[10] H. Wang, E. R. Hawkes, and J. H. Chen, A direct numerical simulation study of flame structure and stabilization of an experimental high Ka CH4/air premixed jet flame, Combustion and Flame 180 (2017) 110–123.

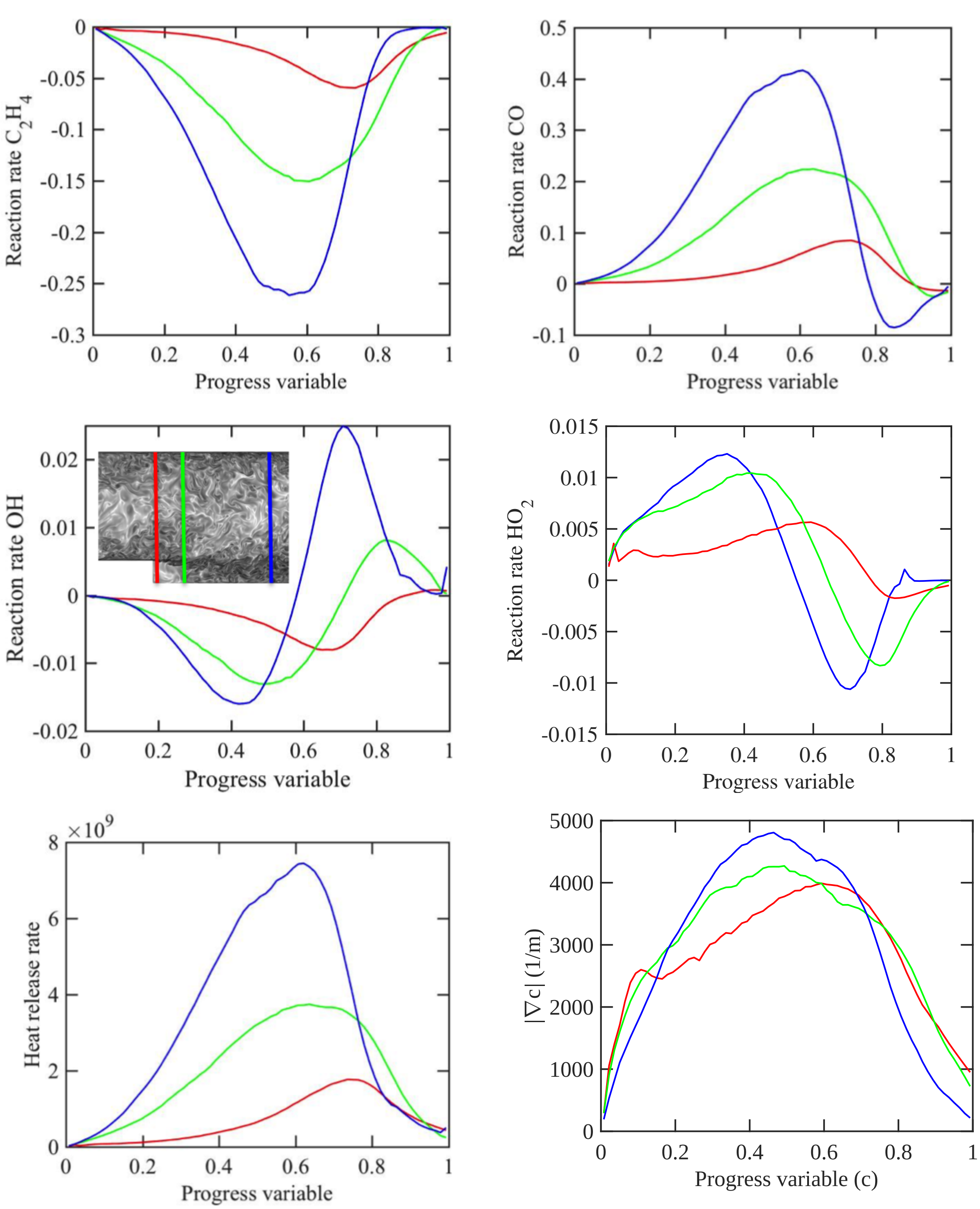

Figure 10: Mean reaction rates of $C_2H_4$, $CO$, $OH$, and $HO_2$, heat release rate and magnitude of the gradient of progress variable conditioned on progress variable at different streamwise locations.